Journal of Power Sources 274 (2015) 318–323

Contents lists available at ScienceDirect

Journal of Power Sources

journal homepage: www.elsevier.com/locate/jpowsour

Effect of the symmetric cell preparation temperature on the activity of $Ba_{0.5}Sr_{0.5}Fe_{0.8}Cu_{0.2}O_{3-\delta}$ as cathode for intermediate temperature Solid Oxide Fuel Cells

Santiago Vázquez [a, b], Juan Basbus [c], Analía L. Soldati [c], Federico Napolitano [c], Adriana Serquis [c], Leopoldo Suescun [a, b, *]

[a] Cryssmat-Lab, Cátedra de Física, DETEMA, Facultad de Química, Universidad de la República, P.O. Box 1157, 11800 Montevideo, Uruguay
[b] Espacio Interdisciplinario, Universidad de la República, José E. Rodó 1843, 11300 Montevideo, Uruguay
[c] Grupo Caracterización de materiales, CAB-CNEA, Bustillo 9500, 8400 Bariloche, Argentina

HIGHLIGHTS

- BSFCu is prepared in one step at 850 °C by a modified gel-combustion route using EDTA.
- The cubic nanocrystalline material is used to prepare symmetrical cells with CGO.
- The effect of the cell preparation temperature on the cathode activity was evaluated.
- The ASR of cells prepared, follows the tendency: $ASR_{900°C} < ASR_{950°C} < ASR_{1000°C}$.
- Cells prepared at 900 °C shows ASR values as low as 0.035 (1) Ω cm^2 at 700 °C.

ARTICLE INFO

Article history:
Received 11 July 2014
Received in revised form
29 September 2014
Accepted 12 October 2014
Available online 18 October 2014

Keywords:
IT-SOFC
Cathode
Gel combustion
XRD
EIS

ABSTRACT

In this work we studied the electrochemical performance of $Ba_{0.5}Sr_{0.5}Fe_{0.8}Cu_{0.2}O_{3-\delta}$ (BSFCu) as cathode for Intermediate Temperature Solid Oxide Fuel Cells (IT-SOFC) with $Ce_{0.9}Gd_{0.1}O_{1.95}$ (CGO) electrolyte and the effect of the symmetric cell preparation temperature on the oxygen reduction reaction (ORR) activity. Symmetrical cells with the configuration BSFCu/CGO/BSFCu were prepared at 900 °C, 950 °C and 1000 °C to perform the electrochemical characterization in the 500–700 °C temperature range. The resultant area specific resistance (ASR) of the cells with different preparation temperatures followed the tendency: $ASR_{900°C} < ASR_{950°C} < ASR_{1000°C}$. The symmetric cell constructed at 900 °C showed ASR values of 0.18, 0.078 and 0.035 Ω cm^2 at 600, 650 and 700 °C respectively, which demonstrated superior electrochemical activities than previous reports. Additional, X-ray diffraction (XRD), scanning and transmission electron microscopies (SEM and TEM) techniques were used to characterize the microstructure of the original and fired BSFCu materials and correlate it with the cell preparation temperature.

1. Introduction

Solid Oxide Fuel Cells (SOFCs) convert hydrogen and hydrocarbon fuels into electricity and heat, through an electrochemical reaction, with high efficiency and low emission of pollutants [1,2]. These devices are considered as one of the most promising candidates for power generation from large stationary plants to small and portable distributed generation applications with superior benefits than other fuel cells. However, the high manufacturing cost and materials long term stability have prevented its commercial viability. Nowadays, one of the research targets for SOFCs is lowering the operation temperature which can improve the lifetime of the cell/stack, allows the use of cheaper interconnecting and structural components (such as stainless steel) and facilitates the gas sealing [3].

The current research target is focused on the development of electrode materials for intermediate temperature SOFCs (so called IT-SOFCs) operated between 500 and 700 °C. Lowering the operating temperature, however, reduces electrode kinetics and increases the interfacial polarization resistances, particularly on the cathode side of the cell. For this reason, a significant effort is being made to prepare cathode materials with high activity for the

* Corresponding author. Cryssmat-Lab, Cátedra de Física, DETEMA, Facultad de Química, Universidad de la República, P.O. Box 1157, 11800 Montevideo, Uruguay.
E-mail address: leopoldo@fq.edu.uy (L. Suescun).

http://dx.doi.org/10.1016/j.jpowsour.2014.10.064
0378-7753/

oxygen reduction reaction (ORR) in this temperature range [4]. The best cathode materials that have been described are based on the simple perovskite structure $ABO_{3-\delta}$, with cation disorder in the A and B sites and a significant proportion of disordered oxygen vacancies. Generally, these materials are mixed ionic–electronic conductors (MIECs) favoring the reduction of the cathode area specific resistance (ASR) [5]. The lowest ASR values have been reported for cathodes with mixed alkali–earths and/or lanthanides in the A site and mixed cobalt and iron in the B site of the perovskite structure such as (Ba,Sr)(Co,Fe)$O_{3-\delta}$ (BSCF) [6–8], (La,Sr)(Co,Fe)$O_{3-\delta}$ (LSFC) [9–13] and $LnBaCo_2O_{5+\delta}$ [14–17].

Unfortunately, these cathode compositions with high cobalt content show large thermal expansion coefficients (TEC), much larger than those of state-of-the-art electrolytes and interconnector materials which are available for IT-SOFC applications (i.e. gadolinia-doped ceria (CGO), (La,Sr)(GaMg)$O_{3-\delta}$ (LSGM), yttria-stabilized zirconia (YSZ) and ferritic stainless steels) limiting the cell lifetime [18]. Moreover, the easy reduction and evaporation, and the high cost of cobalt are also significant issues. For these reasons, several efforts have recently been made to develop cobalt-free cathodes with high electrocatalytic activity for the ORR process, with similar TEC to the other cell components and structural stability in the operation conditions.

Iron-based perovskite $Ba_{0.5}Sr_{0.5}FeO_{3-\delta}$ has also attracted much attention due to its lower TEC and superior structural stability than cobalt-based materials [19]. However, this material presents a lower activity due to the low electrical conductivity and oxygen permeation [20]. Efimov et al. [21] and Zhao et al. [22,23] were the first to report $Ba_{0.5}Sr_{0.5}Fe_{0.8}Cu_{0.2}O_{3-\delta}$ (BSFCu) as a novel cobalt-free perovskite for IT-SOFC. These authors report a high electrical conductivity with a maximum value between 45 and 57 S cm^{-1} at 600 °C, which exceeds the acceptable limit for cathode applications ($\approx$10 S cm^{-1}). Zhao et al. reported a good electrochemical performance with an ASR value of 0.137 Ω cm^2 at 700 °C working with samaria-doped ceria electrolyte (CSO) and a maximum power density of 718 mW cm^2 at 700 °C in a BSFCu/CSO/NiO–CSO cell.

However, the effect of the cell preparation temperature has not been studied for BSFCu and its influence on the cathode activity is poorly discussed in the literature for SOFCs. From our point of view this is a key parameter in the SOFCs construction process that needs to be evaluated in detail, mainly when nanostructure materials are used in the cell. The preparation temperature may affect the grain size of the cathode material and the cathode/electrolyte interface, so it is important to optimize this parameter to achieve high ORR activities that enable SOFCs to operate at lower temperatures.

In this work we studied the electrochemical performance of the $Ba_{0.5}Sr_{0.5}Fe_{0.8}Cu_{0.2}O_{3-\delta}$ as cathode for IT-SOFC and the effect of the symmetric cell preparation temperature on the cathode ORR activity. The materials $Ba_{0.5}Sr_{0.5}Fe_{0.8}Cu_{0.2}O_{3-\delta}$ and $Gd_{0.1}Ce_{0.9}O_{1.95}$ were synthesized by a modified gel-combustion route using EDTA as chelating agent and NH_4NO_3 as combustion promoter. A detailed structural and microstructural characterization of the BSFCu powder was performed by XRD and TEM. The main purpose of this work is to demonstrate that optimizing a parameter often neglected as the cell preparation temperature is important to improve the cathode performance.

2. Experimental

2.1. Preparation of cathode material: $Ba_{0.5}Sr_{0.5}Fe_{0.8}Cu_{0.2}O_{3-\delta}$

Nanocrystalline $Ba_{0.5}Sr_{0.5}Fe_{0.8}Cu_{0.2}O_{3-\delta}$ (BSFCu) powder was synthesized by a modified gel-combustion route using $Ba(NO_3)_2$, $Sr(NO_3)_2$, $Fe(C_5H_7O_2)_2$ and $Cu(NO_3)_2.3H_2O$ (all >99.9%, from Sigma–Aldrich) as metal sources. The synthesis of BSFCu was performed by dissolving stoichiometric amounts of the mentioned compounds in distilled water in a pyrex-glass beaker. Excess EDTA (99.4–100.6 %, Sigma–Aldrich) was added in a 1.1:1 EDTA/metal ion ratio. In this synthesis route the EDTA plays a role as fuel for combustion and chelating agent in the solution. HNO_3 (70%, Sigma–Aldrich) and NH_4OH (28.0–30.0%, Sigma–Aldrich) was also added to form NH_4NO_3 in-situ and promote the combustion of EDTA. An excess of NH_4OH was added until a pH = 10 was obtained to improve chelating power of EDTA. The solution was then heated until self-combustion occurred. The ashes obtained were pressed into 13 mm pellets at 25 MPa and calcined at 850 °C for 3 h with a heating/cooling rate of 5 °C min^{-1} to obtain nanocrystalline BSFCu powder.

2.2. Preparation of electrolyte material: $Ce_{0.9}Gd_{0.1}O_{1.95}$

The $Gd_{0.1}Ce_{0.9}O_{1.95}$ (CGO) electrolyte material was prepared by a conventional gel-combustion route using $Gd(NO_3)_3.6H_2O$, $Ce(NO_3)_3.6H_2O$ as metal sources and citric acid (CA) as fuel with the molar relation CA:CGO of 2:1. In this case NH_4NO_3 (>99%, Sigma Aldrich) was added to promote the combustion of CA in the relation NH_4NO_3:CA = 6:1. The resulting CGO nanopowder was calcined at 1000 °C for 5 h (CGO1000) with a heating/cooling ramp of 5 °C min^{-1} to eliminate carbon residues from the combustion.

2.3. Symmetric cell fabrication

Symmetric cells were prepared using BSFCu and CGO1000 as starting powders. A dense CGO electrolyte pellet was obtained by uniaxially pressing 500 mg of CGO1000 powder under 25 MPa, to form 13 mm diameter and 1.0 mm thick disks and firing them at 1400 °C for 12 h in air atmosphere with a heating ramp of 4 °C min^{-1}.

The cathode was deposited on both electrolyte surfaces by spin-coating using an ink composed by BSFCu powder, ethanol, α-terpineol, polyvinyl butyral and polyvinyl pyrrolidone as indicated by Baqué et al. [13]. After deposition, the pellets were fired at high temperature to achieve good adhesion of the cathode–electrolyte interface. Calcination temperatures of 900, 950 and 1000 °C were selected for different symmetric cells to evaluate the influence of this parameter on the cathode electrochemical performance. The resulting BSFCu electrodes had an active area of 0.565 cm^2.

2.4. Characterization

The phase purity and microstructure of synthesized powders was characterized by X-ray powder diffraction using an in-house diffractometer (Rigaku Ultima IV, operating at 40 kV and 30 mA using Cu$K\alpha$ radiation). Data for the detailed structural characterization of BSFCu sample and oxygen content determination was collected at D10B-XPD beamline of the Brazilian Synchrotron Light Laboratory (LNLS). The beamline is equipped with a 6-circle Huber diffractometer configured for θ–2θ reflection-geometry with a Mythen 1000 linear position sensitive detector (PSD) with a sample to detector distance of 1022 mm. 10 keV X-rays (λ = 1.24155 Å) were used to illuminate the sample that was mounted in a flat holder and rotated at 2 cycles per second during data collection in the 2θ = 10–120° range in steps of 0.5°. The detector, spanning 3°, collected data six times for each 2θ value. Data reduction and averaging were performed to obtain a powder pattern with $2\theta_{min}$ = 8.7°, $2\theta_{max}$ = 121.3° and $2\theta_{step}$ = 0.005°. The pattern was fitted by the Rietveld method [24] using FullProf Suite software and including anomalous scattering (f′ and f″) corrections for all atomic species for 10 keV radiation [25,26].

Morphological characterization of cathode powder was also done by transmission electron microscopy (TEM) using a Philips CM 200 UT device. Cross sectional images of the cathode–electrolyte interphase were performed by scanning electron microscope (SEM) using a Philips 515 equipment.

The area specific resistance (ASR) of BSFCu cathode fired at 900, 950 and 1000 °C in symmetrical cells was determined by electrochemical impedance spectroscopy (EIS) technique in the range 500–700 °C in a 200 ml min^{-1} ambient air flux. These measurements were performed using a potentiostat/impedance analyzer Autolab (Eco Chemie BV) at frequencies from 1 MHz to 3 mHz and an applied voltage amplitude of 10 mV. Zview program was used for data processing and analysis [27].

3. Results and discussion

3.1. Structural and morphological characterization

$Ba_{0.5}Sr_{0.5}Fe_{0.8}Cu_{0.2}O_{3-\delta}$ has a perovskite-type structure that crystallizes in the cubic Pm-3m (#221) space group. In the ideal cubic perovskite structure, the B cations are 6-fold and the A cations 12-fold coordinated, with the oxygen anions. In this compound, however, Basbus et al. [28] reported a presence of ~1/8 oxygen vacant sites ($\delta \approx 0.375$) that reduces the average coordination number of Sr/Ba to 10 and of Fe/Cu to 5 and determines the average charge of Fe/Cu site to be 3.25+. The large number of oxygen vacant sites in a disordered cubic structure allows a high oxygen ion conductivity. The presence of $Fe^{3+/4+}$ and $Cu^{2+/3+}$ in a disordered arrangement in a cubic lattice also ensures electronic conductivity. Fig. 1 shows the synchrotron X-ray powder diffraction pattern of BSFCu compound fitted by the Rietveld method. The refinement, showing a very good visual fit, converged to final R_{wp} and χ^2 values of 7.52 and 1.20 respectively. Table 1 summarizes the results of this analysis where a small amount of CuO (0.54% weight as extracted from the FullProf quantitative phase analysis) was detected showing major peaks at $2\theta = 28.45°$ and 31.0°. The peak broadening in the diffraction pattern was attributed to the small size of the crystallites and was determined using the Scherrer equation as implemented in FullProf with 18.4 nm average crystallite size.

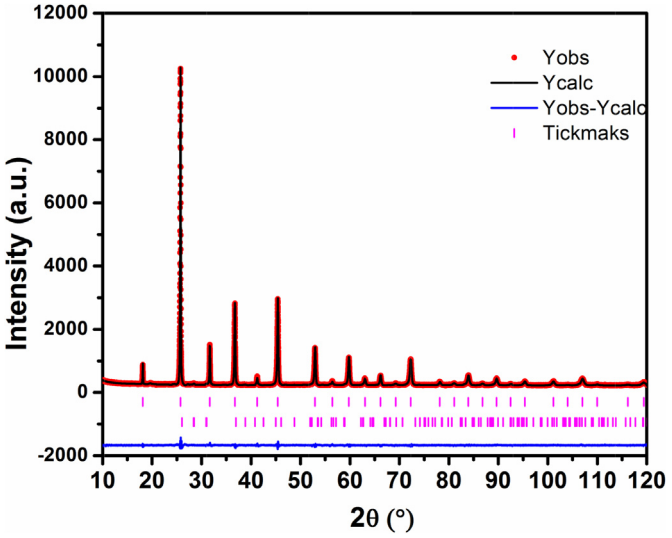

Fig. 1. Rietveld fit of XRD data of as-prepared BSFCu powder. Black dots are observed intensities, the red line is the calculated intensity, vertical bars are peak positions for BSFCu (top) and CuO (bottom) and blue line is the difference between observed and calculated intensities. (For interpretation of the references to color in this figure legend, the reader is referred to the web version of this article.)

Table 1
Final structural parameters of BSFCu extracted from the Rietveld fit.

Space group		$a = b = c = 3.9389$ (1) Å			$\chi^2 = 1.20$	
$Pm\bar{3}m$ (#221)		$\alpha = \beta = \gamma = 90°$			Rp = 10.1	Rwp = 7.52
Atoms	Wyckoff position	*x*	*y*	*z*	Occ.	Biso (Å^2)
Ba	1b	1/2	1/2	1/2	0.5	1.890 (5)
Sr	1b	1/2	1/2	1/2	0.5	1.890 (5)
Fe	1a	0	0	0	0.8	1.853 (8)
Cu	1a	0	0	0	0.2	1.853 (8)
O	3d	0	0	1/2	0.862 (1)	3.41 (3)
Average crystallite size (nm)						18.4 (1)

In order to study the morphology of BSFCu powder before the symmetric cell preparation, TEM images were acquired. Fig. 2 shows the dark and bright field images of agglomerates of BSFCu nanoparticles with sizes between 10 and 100 nm. However the particle size distribution as is shown in the histogram has an exponential decay of particle size with a mean of (119 ± 140) nm. We attribute this exponential decay to an uncontrolled crystal growth process due to the quick and exothermic combustion reaction.

Fig. 2d shows how the crystallite size of the as-prepared BSFCu nanopowder changes with temperature when fired at 900, 950 and 1000 °C for 3 h. The 850 °C XRD pattern represents the starting BSFCu material and the next patterns correspond to the BSFCu material calcined at the symmetric cell preparation temperatures. The decrease in the peak profile width can be associated with a crystal growth process which results in a reduction of the exposed surface of the cathode.

3.2. Electrochemical characterization

The cells with the configuration BSFCu/CGO/BSFCu were investigated via Electrochemical Impedance Spectroscopy (EIS) under open circuit conditions and in air atmosphere from 500 to 700 °C. A cross sectional image of the cathode-electrolyte interface is shown in Fig. 3. A uniform layer of porous cathode with a thickness of 30–40 μm can be observed.

Typical Nyquist plots were obtained and are shown in Fig. 4. The impedance data was corrected by the effective area of the electrode and the symmetrical configuration of the cell $Z = (Z_{exp}A_{electrode})/2$ were Z_{exp} is the measured impedance and $A_{electrode}$ is the area of the deposited electrode.

The Nyquist plots show only the curve due to the ORR; in all the cases there are more than one arc that contributes to the impedance spectra. The ORR mechanism is complex and could involve various determining reaction steps which could be studied using EIS. In our case, for the cells prepared at 900 and 950 °C there are high frequency (HF) and low frequency (LF) arcs, which we associate to the charge transfer process in the surface of the cathode and to the ionic diffusion in the bulk of the material, respectively [29]. The LF contribution seems to loose importance with the cell preparation temperature, disappearing at 1000 °C (Fig. 4), consistently with the increase of bulk volume with crystal growth that produces the reduction of the resistance associated with ionic conduction due to longer continuous diffusion paths within each grain of the cathode material. On the contrary, the HF arc increases its importance with increasing cell preparation temperature. This is consistent with the observed decrease of the total active area for the charge transfer process due to crystal growth at higher temperature (Fig. 2d). However, a better understanding of each mechanism and their influence of the EIS spectra may require a detailed study varying the pO_2 or electrode thickness [30].

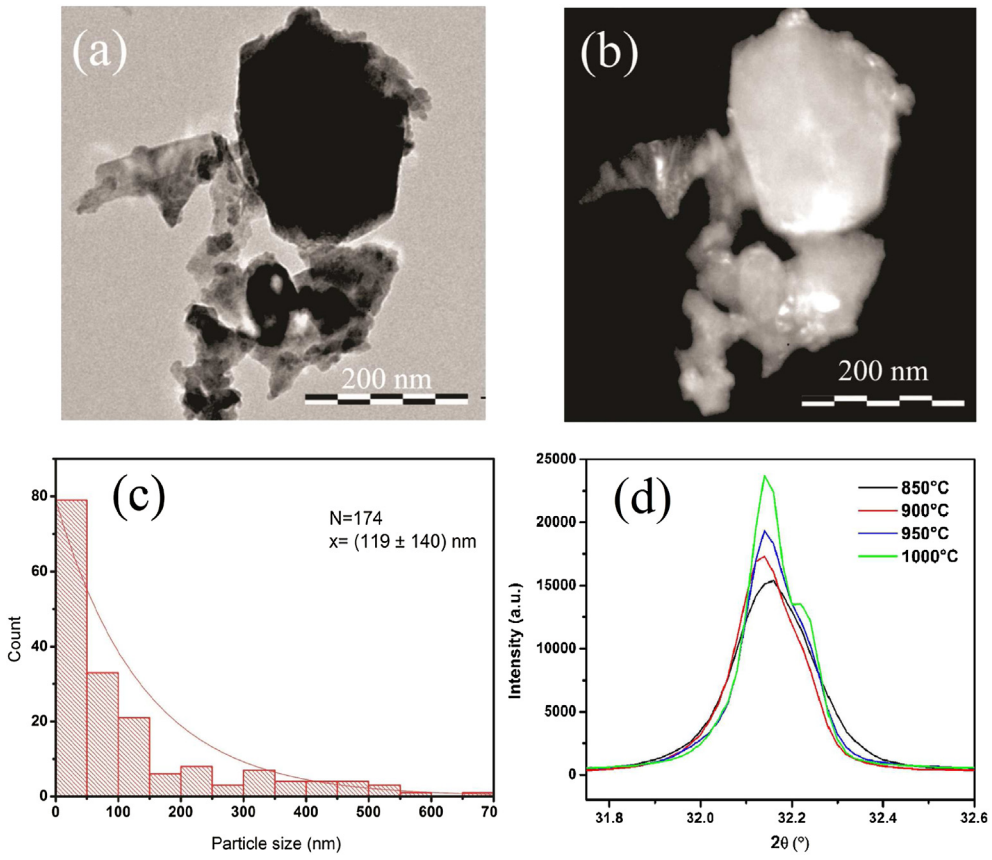

Fig. 2. (a) Dark field and (b) bright field TEM images of a BSFCu particle composed of the aggregate of many crystallites. (c) Histogram of the particle size distribution. (d) XRD analysis of the temperature evolution of the peak (110) of BSFCu between 850 and 1000 °C.

In order to obtain the ASR values we can use the difference between the low-frequency and the high-frequency intercepts with the real axis. To achieve more accurate ASR values, the impedance spectra were fitted to an equivalent circuit shown in Fig. 5a. The circuit is composed by an inductance L due to the current probes, a resistor R_E due to the electrolyte resistance and two constant phase elements (CPE_{HF} and CPE_{LF}) in parallel with resistor (R_{HF} and R_{LF}). Using this model the ASR is easily calculated as $ASR = R_{HF} + R_{LF}$.

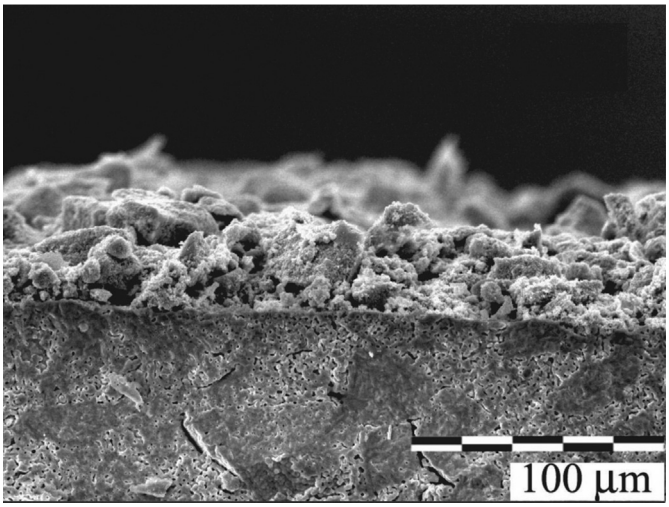

Fig. 3. Cross-section SEM images of the BSFCu/CGO interface, the cathode shows a layer thickness between 30 and 40 µm.

The ASR values are resumed in the Table 2 as a function of the cell preparation temperature and the cell measurement temperature. Arrhenius plot of the ASR is shown in Fig. 5b including previous results from Zhao et al. [22].

The ASR of the symmetric cells prepared at 900, 950 and 1000 °C shows the following tendency $ASR_{900°C} < ASR_{950°C} < ASR_{1000°C}$. This lower cathode activity when the firing temperature is higher can be due to the crystal growth and consequent reaction area loss, so this slows the adsorption and bulk incorporation kinetics of O_2 in the cathode. The corresponding activation energy (E_a) of the Arrhenius plot was determined from the log (ASR) vs. T^{-1} slope and were 132, 113 and 123 kJ mol^{-1} for cathodes fired at 900, 950 and 1000 °C respectively. The obtained activation energies are very similar which indicates an equal rate limiting process for the ORR, result which suggests that the reaction rate increases due to increased reaction surface area of the cathode and not to a change of mechanism.

The lowest ASR values were 0.18, 0.078 and 0.035 Ω cm^2 at 600, 650 and 700 °C respectively, for the symmetric cell prepared at 900 °C. These values are comparable or lower than the required cathode ASR for SOFCs applications (≈0.15 Ω cm^2 [1]) and similar to the best results already reported for $Ba_{0.5}Sr_{0.5}Co_{0.8}Fe_{0.2}O_{3-\delta}$ [7]. For this reason $Ba_{0.5}Sr_{0.5}Fe_{0.8}Cu_{0.2}O_{3-\delta}$ is a cobalt-free material with high electrocatalytic activity that deserves further study as cathode for IT-SOFCs applications working in the 600–700 °C range.

4. Conclusions

We synthesized nanostructured $Ba_{0.5}Sr_{0.5}Co_{0.8}Fe_{0.2}O_{3-\delta}$ cathode material by an alternative gel-combustion route at low

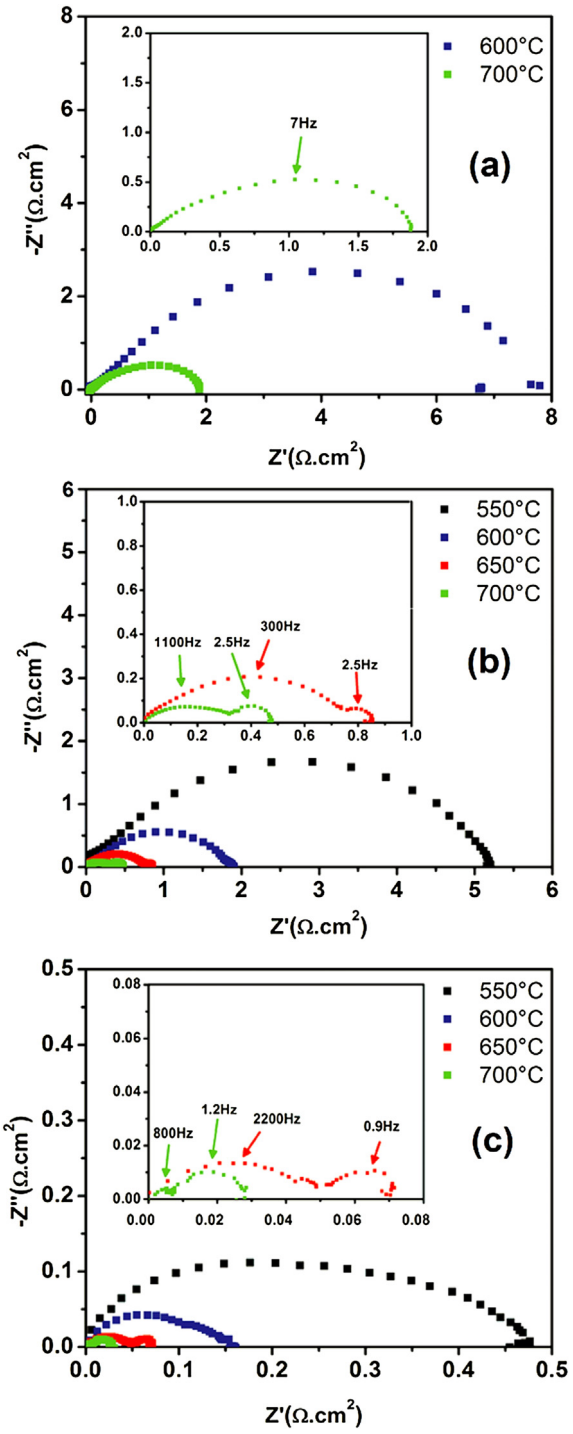

Fig. 4. Nyquist plots in the 1 MHz–3 mHz frequency range for BSFCu/CGO/BSFCu symmetric cells prepared at (a) 1000 °C, (b) 950 °C and (c) 900 °C. 500 °C data was omitted for clarity. See Table 2 for ASR values at 500 °C.

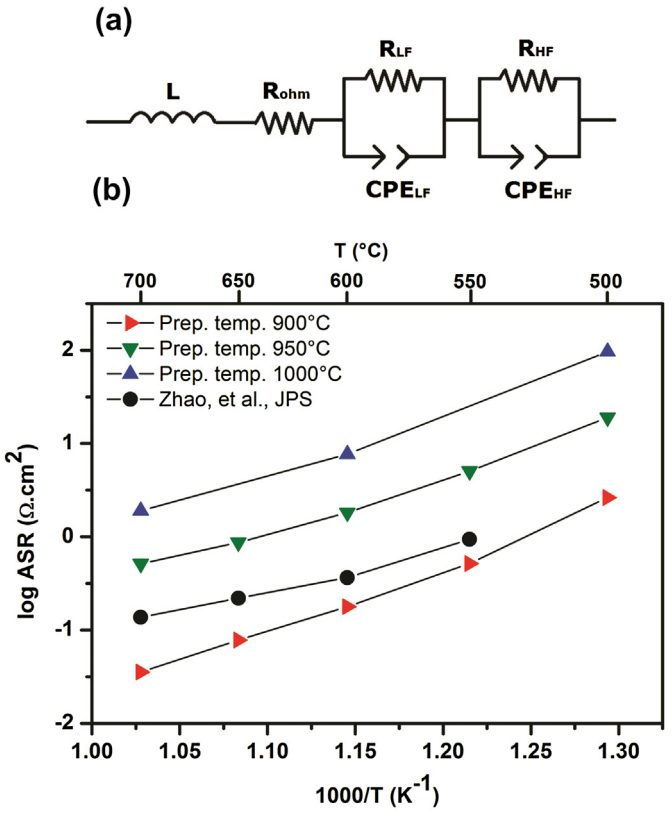

Fig. 5. (a) Equivalent circuit used to fit EIS data for BSFCu/CGO/BSFCu symmetrical cells. (b) Arrhenius plot of ASR for symmetrical cells prepared at 900, 950, 1000 °C and reported values of Zhao et al. [22] for symmetric cells BSFCu/CSO/BSFCu.

Table 2
ASR values obtained for BSFCu/CGO/BSFCu symmetrical cells prepared at 900, 950 and 1000 °C.

T (°C)	ASR (Ω.cm^2)		
	900	950	1000
500	2.6 ± 0.2	18.9 ± 0.3	96.3 ± 0.7
550	0.52 ± 0.06	5.05 ± 0.08	–
600	0.18 ± 0.02	1.81 ± 0.04	7.7 ± 0.5
650	0.078 ± 0.004	0.87 ± 0.01	–
700	0.035 ± 0.001	0.513 ± 0.006	1.9 ± 0.3
E_a (kJ mol^{-1})	123 ± 12	113 ± 7	132 ± 7

temperature. The cathode electrochemical performance was studied as function of the symmetric cell preparation temperature and the cathode ASR was calculated for cells prepared at 900, 950 and 1000 °C. The ORR activity of the $Ba_{0.5}Sr_{0.5}Co_{0.8}Fe_{0.2}O_{3-\delta}$ cathode was enhanced by lowering the symmetric cell preparation temperature ($ASR_{900°C} < ASR_{950°C} < ASR_{1000°C}$). The symmetric cell constructed at 900 °C showed ASR values of 0.18, 0.078 and 0.035 Ω cm^2 at 600, 650 and 700 °C respectively, which demonstrated superior electrochemical activities than previous reports for the BSFCu material.

For the development of IT-SOFCs it is necessary to optimize microstructural characteristics of the materials, and the cell preparation temperature is one of such important parameters to be evaluated that, as we show in this work, may have high influence on the electrochemical activity at the lower temperatures. The low ASR values obtained in this work reinforce the idea that BSFCu is a promising material for IT-SOFC.

Acknowledgments

This work was supported by Agencia Nacional de Investigación e Innovación (Uruguay) through grant FSE_2009_1_51 and Laboratorio Nacional de Luz Synchrotron (LNLS, Campinas, SP, Brazil) through a grant to perform research proposal XRD1-15297 at D10B-XPD beamline. LS is also indebted to PEDECIBA. SV acknowledges the financial support of Espacio Interdisciplinario-Universidad de la República. The authors are grateful to Dr. Alberto Caneiro for the use of his laboratories for symmetrical cell preparation and helpful discussion and to Carlos Cotaro for the SEM images.

References

[1] B.C.H. Steele, A. Heinzel, Nature 414 (2001) 345–352.
[2] E. Perry Murray, T. Tsai, S.A. Barnett, Nature 400 (1999) 649–651.
[3] A. Boudghene Stambouli, E. Traversa, Renew. Sustain. Energy Rev. 6 (2002) 433–455.
[4] Z. Shao, S.M. Haile, Nature 431 (2004) 170–173.
[5] S.B. Adler, Chem. Rev. 104 (2004) 4791–4843.
[6] H. Patra, S.K. Rout, S.K. Pratihar, S. Bhattacharya, Int. J. Hydrogen Energy 36 (2011) 11904–11913.
[7] W. Zhou, R. Ran, Z. Shao, J. Power Sources 192 (2009) 231–246.
[8] B. Liua, Y. Zhanga, L. Zhanga, Int. J. Hydrogen Energy 34 (2009) 1008–1014.
[9] D. Beckel, U.P. Muecke, T. Gyger, G. Florey, A. Infortuna, Ludwig J. Gauckler, Solid State Ionics 178 (2007) 407–415.
[10] D. Marinha, J. Hayd, L. Dessemond, E. Ivers-Tiffée, E. Djurado, J. Power Sources 196 (2011) 5084–5090.
[11] B. Lai, K. Kerman, S. Ramanathan, J. Power Sources 196 (2011) 1826–1832.
[12] L. Baqué, E. Djurado, C. Rossignol, D. Marinha, A. Caneiro, A. Serquis, ECS Trans. 25 (2009) 2473–2480.
[13] L. Baqué, A. Caneiro, M.S. Moreno, A. Serquis, Electrochem. Commun. 10 (2008) 1905–1908.
[14] S. Lü, X. Meng, Y. Ji, C. Fu, C. Sun, H. Zhao, J. Power Sources 195 (2010) 8094–8096.
[15] J. Xue, Y. Shen, T. He, J. Power Sources 196 (2011) 3729–3735.
[16] S. Pang, X. Jiang, X. Li, Q. Wang, Z. Su, Int. J. Hydrogen Energy 37 (2012) 2157–2165.
[17] C. Gaudillère, L. Olivier, P. Vernoux, C. Zhang, Z. Shao, D. Farrusseng, J. Power Sources 195 (2010) 4758–4764.
[18] J. Molenda, K. Swierczek, W. Zajac, J. Power Sources 173 (2007) 657–670.
[19] Z. Chen, R. Ran, W. Zhou, Z. Shao, S. Liu, Electrochim. Acta 52 (2007) 7343–7351.
[20] J. Jung, S.T. Misture, D.D. Edwards, 24 (2010) 261–269.
[21] K. Efimov, T. Halfer, A. Kuhn, P. Heitjans, J. Caro, A. Feldhoff, Chem. Mater. 22 (2010) 1540–1544.
[22] L. Zhao, B. He, X. Zhang, R. Peng, G. Meng, X. Liu, J. Power Sources 195 (2010) 1859–1861.
[23] L. Zhao, B. He, Y. Ling, Z. Xun, R. Peng, G. Meng, X. Liu, Int. J. Hydrogen Energy 35 (2010) 3769–3774.
[24] H.M. Rietveld, J. Appl. Cryst. 2 (1969) 65.
[25] J. Rodríguez-Carvajal, Phys. B 192 (1993) 55.
[26] C.T. Chantler, J. Phys. Chem. Ref. Data 29 (4) (2000) 597–1048.
[27] D. Johnson, Zview, Scribner Associates Inc.
[28] J.F. Basbus, F.D. Prado, A. Caneiro, L.V. Mogni, J. Electroceramics 32 (4) (2014) 311–318.
[29] H. Gu, H. Chen, L. Gao, Y. Zheng, X. Zhu, L. Guo, Int. J. Hydrogen Energy 34 (2009) 2416–2420.
[30] L. Mogni, F. Prado, A. Caneiro, ECS Trans. 6 (2008) 233–243.